

# Organic & Biomolecular Chemistry

Volume 21  
Number 14  
14 April 2023  
Pages 2831-3024

rsc.li/obc



ISSN 1477-0520

## PAPER

View Article Online  
View Journal | View Issue



Cite this: *Org. Biomol. Chem.*, 2023, **21**, 2930

## Carbene-controlled regioselectivity in photochemical cascades†

Mara Di Filippo and Marcus Baumann \*

Received 25th January 2023,  
Accepted 31st January 2023

DOI: 10.1039/d3ob00122a

rsc.li/obc

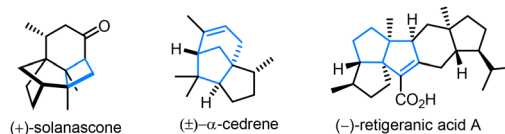
A highly regioselective route to complex carbocyclic scaffolds through a continuous photochemical process is reported. Crucially, we uncovered that *ortho* substituents on the right-hand aryl ring are placed away from a transient carbene species which induces the exclusive regioselectivity observed. By varying the non-symmetrically substituted aryl moiety, we demonstrate how the product outcome favors cyclobutenes for electron-poor and neutral substituents and cycloheptatrienes for more electron-rich systems. Additionally, a photochemically induced rearrangement was uncovered for highly electron-rich substrates that ultimately generates complex hydroperoxides. Overall, this facile one-step process is fast and high yielding and demonstrates the power of photochemistry towards the exploration of new chemical space.

The efficient generation of complex scaffolds that are rich in three-dimensional features continues to be of great importance in medicinal chemistry.<sup>1</sup> This is clearly visible over the last decades whereby aryl rings are frequently replaced by new and diverse isosteres such as bicycloalkanes to improve pharmacokinetic properties of the corresponding drugs.<sup>2</sup>

The use of photochemical processes to bring about the rapid generation of complex biologically active architectures<sup>3</sup> has a longstanding history with notable applications seen in the synthesis of natural products and their precursors (Fig. 1), including (+)-solanascene,<sup>4</sup> (±)-α-cedrene<sup>5</sup> and (–)-retigeranic acid A.<sup>6</sup> The use of light aids in generating highly reactive intermediates upon photoexcitation and often provides benefits such as orthogonality to existing functional groups. Ubiquitous functionalities such as alkenes and carbonyls offer thereby streamlined entries to a variety of substrates that often undergo a multitude of elementary transformations as part of a photochemical cascade process. Recently, LEDs have emerged as replacements for classical metal vapor lamps to trigger valuable chemical transformations, both in applications involving photoredox catalysis as well as the direct excitation of suitable substrates.<sup>7</sup> High-power LEDs emitting in both the visible and UV-A spectrum are now easily integrated in standardized reaction set-ups facilitating both batch<sup>8</sup> and continuous flow<sup>9</sup> applications. The latter thereby holds

promise in providing a simple means to scale photochemical reactions by using appropriate flow reactor set-ups.<sup>10</sup>

We recently reported an intriguing photochemical cascade to create complex pentacyclic scaffolds (5) upon irradiation of alkyne-bearing chalcones (1) with UV-A light (Scheme 1, top).<sup>11</sup> This process was facilitated by a continuous flow set-up that allowed to easily generate gram quantities of product while providing uniform irradiation of the internal tubular reactor. Importantly, the flow approach afforded the targets in short residence times (5–10 min), and cycloheptatriene species (4) were accessed and characterised as late-stage intermediates through minor process modifications. A mechanistic rationale supported by computations was presented that featured a carbene (2) as the key intermediate whose reaction pathway included a postulated norcaradiene intermediate (3). Initial explorations on the reaction scope had indicated that the cascade process is general and allows for variation of several substituents on the left-hand aryl ring as well as the alkyne moiety. In this current study we wish to report on the effect of non-symmetrical substitution on the unexplored right-hand aryl ring and its effects on the regioselectivity of this intriguing



photochemical approach provides for:

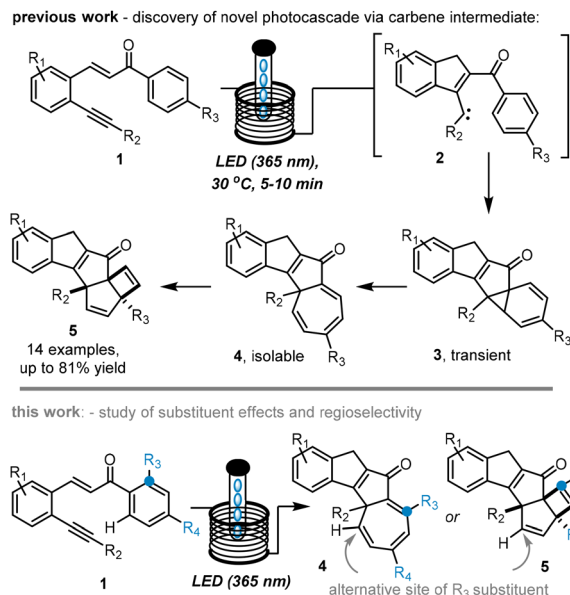
- access to complex polycyclic scaffolds
- high step- and atom-economy
- diverse products from simple substrates
- reagentless approach minimises waste

Fig. 1 Bioactive structures generated photochemically.

University College Dublin, School of Chemistry, Science Centre South, Belfield, Dublin 4, Ireland. E-mail: marcus.baumann@ucd.ie

†Electronic supplementary information (ESI) available: Experimental procedures, spectroscopic data, and copies of NMR spectra. CCDC 2201533–2201535. For ESI and crystallographic data in CIF or other electronic format see DOI: <https://doi.org/10.1039/d3ob00122a>





**Scheme 1** Reaction discovery (top) and regioselectivity hypothesis for *ortho*-substituents (bottom).

cascade. Specifically, we hypothesised that *ortho*-aryl substituents may provide a means to affect or even control the overall regioselectivity by interacting with the postulated carbene intermediate *via* steric or electronic effects (Scheme 1, bottom).

Our study commenced by preparing a selection of suitable substrates *via* aldol condensation and Sonogashira cross coupling reactions from commercial *ortho* iodobenzaldehydes (see ESI† for details). We thereby focused on a single alkyne unit (derived from 1-hexyne) and two left-hand aryl scaffolds, namely a plain benzene unit and a methylenedioxy system (Fig. 2, top). Our previous work had indicated that the right-hand aryl unit tolerates different substituents in its *para* position (*i.e.*, H, alkyl, F, OMe *etc.*). We thus decided to pair these *para* substituents with electronically differentiated *ortho* substituents (*i.e.*, F, Me, OMe) giving two series of substrates varying on the left-hand aryl decoration.

These substrates were subjected to the original photochemical conditions using a high-power LED (365 nm, adjusted to 70 W input power) in combination with a Vapourtec flow reactor and its UV150 module. Solutions of the above substrates (30 mM, MeCN) were pumped through the photo-flow set-up with a residence time of 7 minutes. Using the 2,4-difluoroaryl system generated the respective photo-products **5a** and **5b** in good chemical yields whilst observing full conversion of substrates. The presence of the cyclobutene system was established using <sup>1</sup>H and <sup>13</sup>C NMR spectroscopy (incl. HSQC and HMBC). Notably, the crude reaction mixture showed only one product whose regiochemistry could be established unambiguously through securing a crystal structure of **5b** (Fig. 2).<sup>12</sup> Next, the analogous 2,4-dimethylbenzene system was subjected to the same conditions and gave a similar outcome as the cyclobutene product (Fig. 2, **5c** and **5d**) was

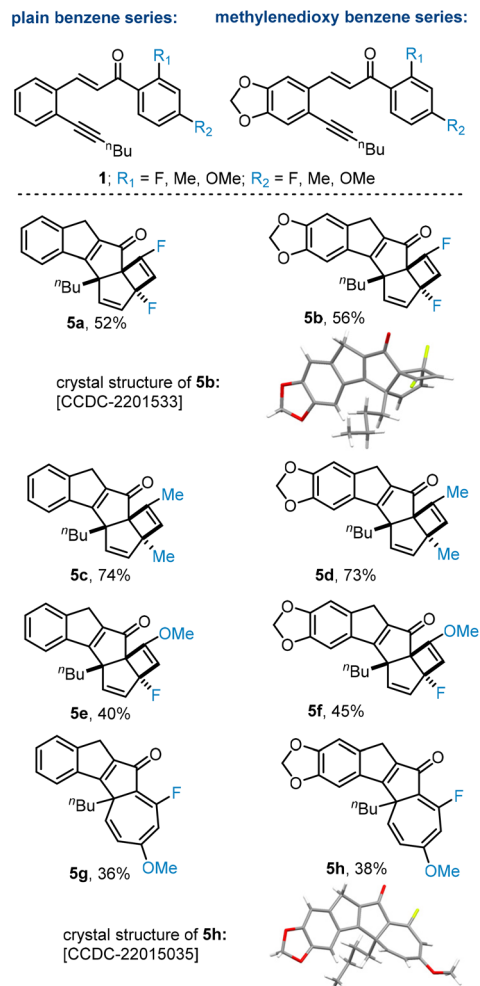


**Fig. 2** Reaction outcome for different aryl systems.

formed in high yield and as a single regioisomer. Crucially, in both cases the regioisomer that has the *ortho*-substituent adjacent to the carbonyl (*i.e.*, away from the intermediate carbene) was obtained. The yields were higher for the products derived from the dimethylbenzene scaffold indicating potential degradation in case of the analogous difluoro species (**5a** and **5b**).

For mono-substituted aryl systems a methoxy substituent in the *para* position leads to the isolation of the cycloheptatriene scaffold (Fig. 3, **5i**, **5j**). As part of this study, we also investi-

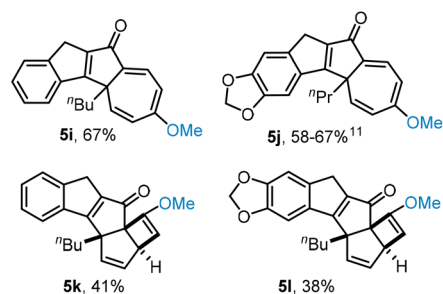


**Fig. 3** Regioselective formation for mono-methoxy systems.

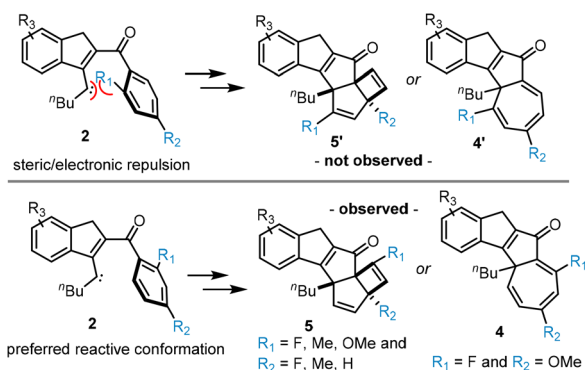




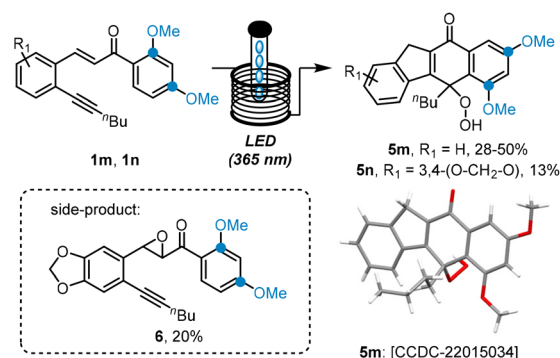
gated the reaction outcome when having a single methoxy group in the *ortho* position which was found to give the cyclobutene scaffold irrespective of the left-hand aryl system (**5k**, **5l**).

To expand on these results, we next evaluated cases possessing both fluoride and methoxy substituents in the respective *ortho* and *para* positions (Fig. 2, bottom). This led to an interesting observation that the cyclobutene species is generated when fluoride is in the *para* position (methoxy in *ortho* position, e.g., **5e** and **5f**) whereas the cycloheptatriene system results when fluoride is in the *ortho* position and the methoxy group in the *para* position (**4g**, **5h**). Assignment of these structures was again aided by advanced NMR techniques, X-ray crystallography (e.g., **5h**) and comparison of key data between these structures. Importantly, the same regioselectivity as highlighted in all the above cases was observed pointing toward a general underlying cause (*vide infra*). We believe that the preference for the cycloheptatriene products **5g** and **5h** is a result of the lower energy transition state and the reduced stability of the corresponding cyclobutene products which favours reversibility in the last step as outlined in our initial study.<sup>11</sup> A key aspect of this work concerned the exclusive regioselectivity observed in forming all cyclobutene and cycloheptatriene species. We propose that in case of fluoride and methoxy groups in the *ortho* position electronic repulsion between the lone pairs on fluorine and oxygen and the carbene favours a reactive conformation whereby these groups are pushed away from the electron density surrounding the carbene intermediate (Scheme 2, top). Conversely, when a methyl group is placed in the *ortho* position an unfavourable steric interaction between the methyl group and the carbene moiety will result in the same conformational bias. As depicted in Scheme 2, this will favour formation of products having the original *ortho* substituent adjacent to the carbonyl group which agrees with the experimental data.

A crucial set of substrates having methoxy groups in both the *ortho*, and *para* positions was studied next. In both cases an unexpected outcome was observed as neither the cycloheptatriene, nor the cyclobutene species was generated. Single crystal X-ray diffraction revealed that a very different scaffold was formed in which the dimethoxybenzene ring was pre-



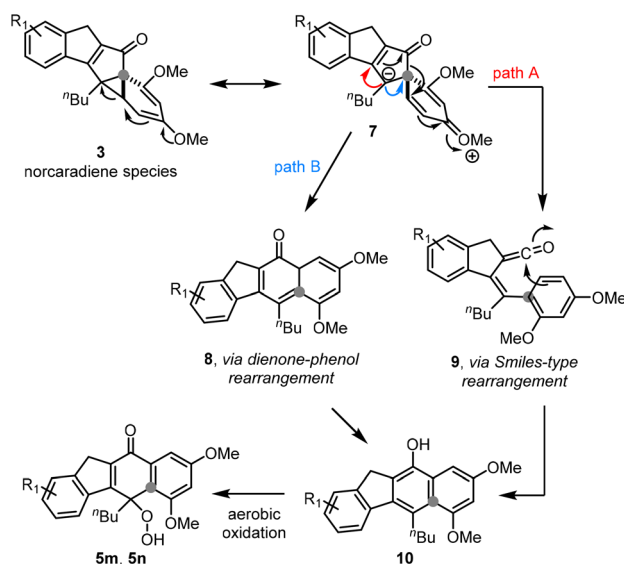
**Scheme 2** Regioselectivity via steric or electronic repulsion between carbene and *ortho* substituents.



**Scheme 3** Reaction outcome for substrates **1m** and **1n**.

served (**5m**, **5n**, Scheme 3). Additionally, a hydroperoxide moiety attached to a fusing cyclohexadienone ring was observed clearly showcasing the unique effect resulting from two electron-donating groups on the right-hand aryl ring. A last feature clearly displayed in the crystal structure is that the substitution pattern of this aryl ring is that of a 3,5-dimethoxy system (relative to the carbonyl) rather than the original 2,4-dimethoxyphenyl arrangement indicating that the C–C bond between carbonyl and aromatic ring is fragmented during this new photo rearrangement. This surprising finding was successfully reproduced giving the indicated product in yields of 13–50% along with unreacted substrate (*ca.* 10% *E*- and 20% *Z*-isomer) as well as an epoxide derivative of the substrate (**6**, *ca.* 20%). As the use of degassed and non-degassed stock solutions rendered the same hydroperoxide product, it is surmised that the peroxidation occurs last in this cascade process whereby a suitable position is undergoing aerobic oxidation irrespective of the photochemical conditions.

The unprecedented nature of these results prompted us to consider possible options for the underlying reaction mechanism (Scheme 4). We thereby propose that under the reaction



**Scheme 4** Proposed mechanistic pathways towards **5m** and **5n**.



conditions the transient norcaradiene species **3** undergoes ring opening assisted by either of the methoxy groups.<sup>13</sup> The resulting oxocarbenium **7** may then undergo a Smiles-type rearrangement (path A) or a dienone-phenol rearrangement (path B) giving after tautomerisation the electron-rich naphthol **10** which is readily oxidised to the hydroperoxide products **5m** and **5n**.<sup>14</sup>

Although photochemically triggered Smiles rearrangements are known in the literature,<sup>15</sup> these are typically based on aryl sulfonamides or sulfonates that extrude SO<sub>2</sub> during the process<sup>16</sup> making the presented case a very unusual example. This proposed Smiles-like process may proceed *via* stepwise formation of a ketene followed by arylative C–C bond formation. Crucially, this also causes the apparent relocation of the methoxy groups to resemble the aforementioned 3,5-disubstitution pattern. The alternative dienone-phenol rearrangement is well preceded under thermal conditions<sup>17</sup> and may also be operational under the photochemical conditions of this flow process. Further studies will be necessary to establish whether one or even both reaction pathways are in operation.

## Conclusions

In summary, we report the regioselective synthesis of complex polycyclic architectures *via* an efficient photo-cascade process. Exploiting a continuous flow set-up provided short reaction time along with high reproducibility. When subjecting a set of 2,4-disubstituted aryl systems to this photochemical process the desired targets were obtained with exclusive regioselectivity in yields up to 74%. It is proposed that the regioselectivity originates from both the electronic and steric repulsion between the *ortho* substituent and a transient carbene intermediate which therefore controls the observed selectivity. For substrates bearing a 2,4-dimethoxyaryl moiety an unprecedented polycyclic hydroperoxide product was obtained in good yield which is believed to be formed either *via* a photo-induced Smiles rearrangement or a dienone-phenol rearrangement. These findings demonstrate how new chemical space can be accessed *via* operationally simple photocascade processes that ultimately render complex targets with diverse chemical scaffolds in a single step.

## Author contributions

Experimental work and data analysis (MDF), writing manuscript (MDF and MB), project supervision and securing funding (MB).

## Conflicts of interest

There are no conflicts to declare.

## Acknowledgements

We are grateful to Dr Helge Mueller-Bunz and Dr Andrew D. Philips (both UCD) for solving the crystal structures reported. Dr Yannick Ortin is thanked for assistance with NMR experiments. MDF wishes to thank the School of Chemistry at University College Dublin for provision of a Sir Walter Hartley Scholarship. Financial support by SFI (20/FFP-P/8712 and 12/RC2275\_P2) and the Royal Society of Chemistry (Research Enablement grant E20-2998) is gratefully acknowledged.

## References

- 1 F. Lovering, J. Bikker and C. Humblet, *J. Med. Chem.*, 2009, **52**, 6752; K. E. Prosser, R. W. Stokes and S. M. Cohen, *ACS Med. Chem. Lett.*, 2020, **11**, 1293; J. Meyers, M. Carter, N. Y. Mok and N. Brown, *Future Med. Chem.*, 2016, **8**, 1753.
- 2 J. M. Anderson, N. D. Measom, J. A. Murphy and D. L. Poole, *Angew. Chem., Int. Ed.*, 2021, **60**, 24754; K. Dhake, K. J. Woelk, J. Becica, A. Un, S. E. Jenny and D. C. Leitch, *Angew. Chem., Int. Ed.*, 2022, **61**, e202204719; R. E. McNamee, A. L. Thompson and E. A. Anderson, *J. Am. Chem. Soc.*, 2021, **143**, 21246.
- 3 M. D. Kärkäs, J. A. Porco Jr. and C. R. J. Stephenson, *Chem. Rev.*, 2016, **116**, 9683.
- 4 A. Srikrishna and S. S. V. Ramasastry, *Tetrahedron Lett.*, 2005, **46**, 7373.
- 5 P. A. Wender and J. J. Howbert, *J. Am. Chem. Soc.*, 1981, **103**, 688.
- 6 P. A. Wender and S. K. Singh, *Tetrahedron Lett.*, 1990, **31**, 2517.
- 7 N. Holmberg-Douglas and D. A. Nicewicz, *Chem. Rev.*, 2022, **122**, 1925; S. P. Pitre and L. E. Overman, *Chem. Rev.*, 2022, **122**, 1717; A. Bonner, A. Loftus, A. C. Padgham and M. Baumann, *Org. Biomol. Chem.*, 2021, **19**, 7737; J. P. Knowles, L. D. Elliott and K. I. Booker-Milburn, *Beilstein J. Org. Chem.*, 2012, **8**, 2025; E. B. Corcoran, F. Levesque, J. P. McMullen and J. R. Naber, *ChemPhotoChem*, 2018, **2**, 931; O. M. Griffiths and S. V. Ley, *J. Org. Chem.*, 2022, **87**, 13204.
- 8 C. Le, M. K. Wismer, Z.-C. Shi, R. Zhang, D. V. Conway, G. Li, P. Vachal, I. W. Davies and D. W. C. MacMillan, *ACS Cent. Sci.*, 2017, **3**, 647.
- 9 L. Buglioni, R. Raymenants, A. Slattery, S. D. A. Zondag and T. Noël, *Chem. Rev.*, 2022, **122**, 2752; C. A. Hone and C. O. Kappe, *Chem.: Methods*, 2021, **1**, 454.
- 10 K. Donnelly and M. Baumann, *J. Flow Chem.*, 2021, **11**, 223; C. Sambiago and T. Noël, *Trends Chem.*, 2020, **2**, 92; T. H. Rehm, *Chem. – Eur. J.*, 2020, **26**, 16952.
- 11 M. Di Filippo, C. Trujillo, G. Sánchez-Sanz, A. S. Batsanov and M. Baumann, *Chem. Sci.*, 2021, **12**, 9895.
- 12 Data of all crystal structures were deposited with CCDC and are available from <https://www.ccdc.cam.ac.uk/>; **5b** – CCDC 2201533; **5h** – CCDC 2201535; **5m** – CCDC 2201534.



- 13 For a related example of methoxyaryl-derived norcaradienes dynamically undergoing ring-opening, please see: A. R. Maguire, P. O'Leary, F. Harrington, S. E. Lawrence and A. J. Blake, *J. Org. Chem.*, 2001, **66**, 7166.
- 14 H. Greenland, J. T. Pinhey and S. Sternhell, *Aust. J. Chem.*, 1987, **40**, 325; M. J. Cabrera-Afonso, S. R. Lucena, Á. Juarraz, A. Urbano and M. C. Carreño, *Org. Lett.*, 2018, **20**, 6094.
- 15 For recent reports on photochemical Smiles rearrangements, please see: G. G. Wubbels, N. Ota and M. L. Crosier, *Org. Lett.*, 2005, **7**, 4741; C. A. Lawson, A. P. Dominey, G. D. Williams and J. A. Murphy, *Chem. Commun.*, 2020, **56**, 11445.
- 16 For recent reports on photochemical Smiles rearrangements, based on sulfonamides and sulfonates please see: C. Hervieu, M. S. Kirillova, T. Suárez, M. Müller, E. Merino and C. Nevado, *Nat. Chem.*, 2021, **13**, 327; D. M. Whalley, H. A. Duong and M. F. Greaney, *Chem. Commun.*, 2020, **56**, 11493; D. M. Whalley, H. A. Duong and M. F. Greaney, *Chem. – Eur. J.*, 2019, **25**, 1927; J. J. Douglas, H. Albright, M. J. Sevrin, K. P. Cole and C. J. R. Stephenson, *Angew. Chem., Int. Ed.*, 2015, **54**, 14898.
- 17 K. Hata, H. Hamamoto, Y. Shiozaki, S. B. Cämmerer and Y. Kita, *Tetrahedron*, 2007, **63**, 4052; B. Miller, *Acc. Chem. Res.*, 1975, **8**, 245.

